Supporting Information

Rationalizing the Phase Behavior of Triblock-Copolymers through Experiments and Molecular Simulations

Germán Pérez-Sánchez[1,], Filipa A. Vicente[1], Nicolas Schaeffer[1], Inês S. Cardoso[1], Sónia P. M. Ventura[1], Miguel Jorge[2] and João A. P. Coutinho[1,*]*

[1]CICECO, Departamento de Química, Universidade de Aveiro, 3810-193 Aveiro, Portugal

[2]Department of Chemical and Process Engineering, University of Strathclyde, 75 Montrose Street, Glasgow G1 1XJ, United Kingdom

[*]Corresponding authors

Campus Universitário de Santiago, University of Aveiro, Aveiro, Portugal

Tel: +351-234-370200; Fax: +351-234-370084; E-mail addresses: gperez@ua.pt, jcoutinho@ua.pt

Section S1 - Model Validation

The study performed by Hezaveh et al.[1] for Pluronics in 1,2-dimyristoyl-sn-glycero-3-phosphocholine (DMPC) lipid bilayers served as the initial reference for the model developed in this work. Their CG model parameters were based on All-Atom MD simulations with diverse PEG and PPG chain lengths in water. The radius of gyration (Rg) was selected as the reference property to calibrate the bonded and non-bonded parameters. They obtained parameters for adjusted "SC3" and "SP1" MARTINI beads to map the PPG and PEG chains, respectively. The non-bonded and bonded interactions selected by Hezaveh et al.[1] are shown in **Tables S1** and **S2**, respectively.

In this work, the original SP1 and SC3 MARTINI parameters for PPG and PEG are maintained in conjunction with the bonded parameters from Hezaveh et al.[1] This mapping was able to correctly reproduce (i) the complexity of the formation of cross-linked micelles in reverse Pluronics and (ii) a reasonable agreement in the micelle size distribution over all Pluronics. Our proposed model was compared against other CG models for Pluronics available in the literature, namely the models of Hakateyama et al.,[2] Hezaveh et al.[1] and Nawaz et al.[3,4] Accurate description of Pluronic micelle size and shape was the reference criterion for comparison. Dynamic Light Scattering (DLS) measurements (Malvern Zetasizer Nano-ZS) were carried out to obtain a reference for the micelle size distribution under the same concentration and temperature conditions as in the MD simulations. Each system was analyzed a minimum of five separate times over a 2 hr period to ensure the formation of stable aggregates, with the average aggregate size reported. All measurements were performed using ultrapure water and left to equilibrate for 30 min at the tested temperature prior to measurements.

Table S1. Lennard-Jones non-bonded interaction parameters for the models tested in this work. PEG, PPG and W are polyoxyethylene glycol, polyoxypropylene glycol and water, respectively.

Models	PEG-PEG		PEG-PPG		PPG-PPG		PEG-W		PPG-W	
	ε (kJ/mol)	σ (nm)	ε (kJ/mol)	σ (nm)	ε (kJ/mol)	σ (nm)	ε (kJ/mol)	σ (nm)	ε (kJ/mol)	σ (nm)
This work	3.38	0.43	2.62	0.47	2.62	0.43	4.50	0.47	2.70	0.47
Hezaveh	3.50	0.48	2.90	0.47	2.60	0.50	4.50	0.47	3.50	0.47
Hakateyama	4.20	0.47	3.40	0.47	2.60	0.47	3.40	0.47	1.80	0.47
Nawaz	3.37	0.43	2.62	0.43	2.81	0.43	4.25	0.47	3.5	0.47

Table S2. Bonded interactions for the models presented in **Table S1**.

	PEG				PPG			
	bond		angle		Bond		angle	
	b_B (nm)	K_B (kJ/mol.nm^2)	θ_A (degrees)	K_A (kJ/mol)	b_B (nm)	K_B (kJ/mol.nm^2)	θ_A (degrees)	K_A (kJ/mol)
This work	0.28	8000	155	40	0.28	5000	155	40
Hezaveh	0.28	8000	155	40	0.28	5000	155	40
Hakateyama	0.47	1250	180	25	0.47	1250	180	25
Nawaz	0.265	17000	115	50	0.335	17000	120	50

Two different Pluronics, one reverse 10R5 and one normal L-35, were considered for model comparison purposes. This selection was motivated by the fact that both Pluronics have the same PPG and PEG content and similar molecular weights (~ 2000). Although both Pluronics possess a similar micelle size, they exhibit two very different micelle crowns, which results in a significant deviation in their inter-micelle interactions and thermo-response behavior. The capacity to capture this subtle difference between normal and reverse Pluronics is a crucial test of any CG model. The Pluronic concentration was set to 5 wt% under room temperature conditions. All the MD simulations were carried out in cubic boxes with 30 Pluronic chains for 1 μs of simulation time. Unless otherwise stated, the MD simulation protocol carried out in the main manuscript was followed in this test. **Figure S1** shows the MD snapshots with the final micellar conformation for both the 10R5 and L-35 Pluronics systems.

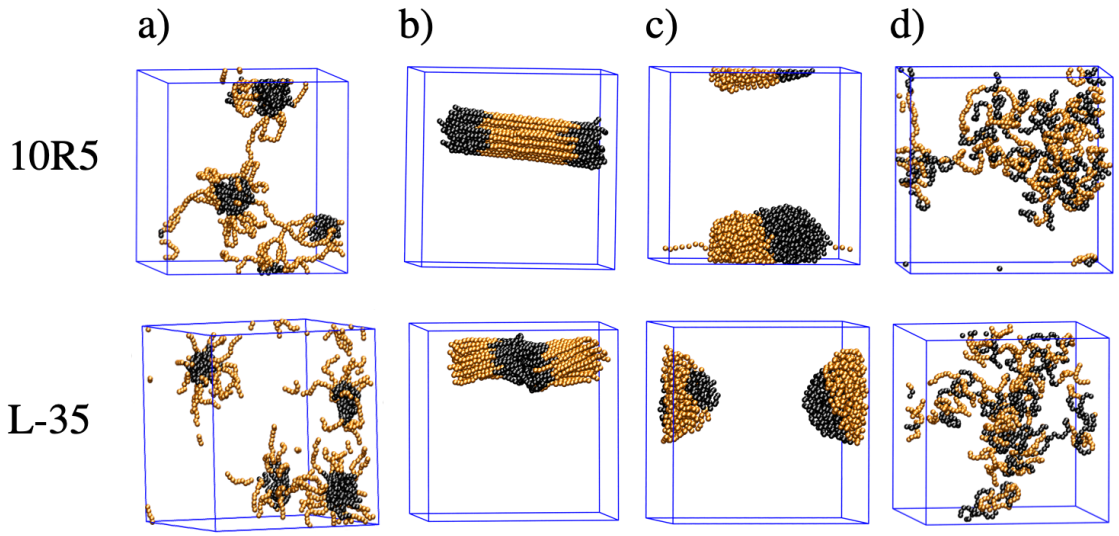

Figure S1. MD simulation snapshots after 1 μs of simulations time for 10R5 (top) and L-35 (bottom). a) the model developed in this work, b) Hezaveh,[1] c) Hakateyama[2] and d) Nawaz.[3,4]

Important differences were found in the micelle formation after 1 μs of simulation time between the different models. Our model (a) yielded 3 micelles with an aggregation number of 10 Pluronic chains per micelle in 10R5 and L-35. This leads to a micelle diameter in good agreement with experimental results as shown in **Table S3**. Furthermore, it accurately captured the characteristic micelle shape of reverse and normal Pluronics (flower petal-like and star-like shapes) as well as the phase behavior with both Pluronics in the homogeneous phase as one expects below the cloud point temperature. No other models were able to reproduce all benchmark criteria. For both Pluronics, all models were incapable to reproduce the proper micelle distribution, furthermore, the Nawaz model (d) was even unable to produce micelles after 1 μs. It must be noticed that the atomistic details included in this model for Pluronics, such as specific dihedrals to reproduce the atomistic radius of gyration, hardly affected the dynamics of the system and made impossible to use the regular CG simulation time step of 10 fs; instead, an atomistic MD time step of 5 fs was used. A brief view of (b) and (d) models strongly suggests that the PPG bead interactions are too hydrophilic – thus lack a driving force for chain aggregation and micelle core formation. The fact that the Nawaz model (d) does

not form aggregates while the Hezaveh model (b) forms rather unphysical bundles of chains, is likely due to the relatively stronger inter-chain attraction energies in the latter (see Table S1). The Hakateyama model (c) did produce aggregates, but these were quite large compared with the experimental data found in the literature for 10R5 micelles[5] as well as experimental results carried out in our laboratory (**Table S3**). Importantly, these aggregates showed an unrealistic structure, with both the PPG and the PEG moieties forming individual aggregates and leading to incipient phase separation. The results shown in (c) suggest that both PEG and PPG beads are too hydrophobic, which leads to the phase separation. Bearing in mind that all the simulated systems were run well below the cloud point of both Pluronics, the phase separation observed in the Hakateyama model is unrealistic.

One of the main problems that a computational model has to face is whether it can reproduce the experimental micelle size distribution. The micelle formation is a complex process which first involves the Pluronic self-assembly (hydrophobic and hydrophilic balance) followed by inter-micelle interactions in later stages. Thus, six MD simulations containing 60 Pluronics (5 wt%) in water were performed to analyze the micelle distribution of the six Pluronics involved in this work, which are presented in **Figure 1** in the main manuscript. The temperature in the MD simulations was well below the cloud point temperature in all cases to ensure that the systems are in the homogeneous regime. The protocol followed in the MD simulations was the same as the MD simulations carried out in the main manuscript. The cluster counting code was used to obtain the micelle density profiles which were used to estimate the micelle diameter. Subsequently, the experimental micelle size distributions of the six Pluronics were obtained in our laboratory by DLS measurements at 25ºC or below according to the protocol previously

presented. The micelle size distribution was not measured in L-61 since it is not soluble at concentrations > 2.5 wt%. The results are shown in **Table S3**.

Table S3. Experimental (DLS) and computational (MD) micelle size diameters ∅ (nm) for 10R5, 17R4, 31R1, L-31, L-35 and L-61 in aqueous solution at 5 wt% concentration. The temperature was fixed at 25ºC, except for 31R1 (10ºC) and L-35 (15ºC), in both experiments and simulations. The symbol >> means that a noticeable number of micelles above the average micelle size were found in the DLS measurements. Na*is Na × number of PPG segments.

	10R5	**17R4**	**31R1**	**L-31**	**L-35**	**L-61**
Exp.	2.30	3.44	2.2 >>	1.78 >>	2.51 >>	—
MD	2.94	4.0	4.14	3.00	3.16	3.40
Na*	112	168	260	160	112	210

It must be highlighted that the poly-dispersity inherent to Pluronics[6,7] yields a large micelle size range. However, the values shown in **Table S3** are in very reasonable agreement with those found in the MD simulations, especially when Na^* is < 150, *i.e.*, when the PEG/PPG ratio approaches one. The most important feature of our MD approach is that it can describe fairly well the micelle crown shape and, consequently, properly reproduce the inter micelle interactions, an important aspect to study thermo-responsive systems such as Pluronics aqueous solutions.

Table S4. Densities, ρ (kg·m^3), enthalpies of vaporization, ΔH_{vap} (kJ·mol), and free energies of hydration, dG_{sol} (kJ·mol), obtained in the MD simulations using our approach and the models shown in **Figure S1**. Unless otherwise stated, the MD calculations were carried out at ambient pressure and temperature. PEG and PPG are polyoxyethylene glycol and polyoxypropylene glycol single units (monomers) whereas PEG2 and PPG2 are double chain units (dimers).

	This work			Hakateyama			Hezaveh			Nawaz			Experimental reference		
	ρ	ΔH_{vap}	dG_{sol}	ρ	ΔH_{vap}	dG_{sol}	ρ	ΔH_{vap}	dG_{sol}	ρ	ΔH_{vap}	dG_{sol}	ρ	ΔH_{vap}	dG_{sol}
*PEG	772	–	-16.57	627	–	-4.87	547	–	-16.56	768	–	-13.74	729[8]	–	-8.03[9]
PPG	823	–	2.52	767	–	10.26	440	–	-5.00	810	–	-5.01	692[8]	–	n/a
PEG2	1032	41.22	-39.32	671	39.46	-9.30	798	41.44	-39.30	1061	42.25	-35.42	860[8,10,11]	34.47[12]	-20.25[9]
PPG2	1334	35.45	-5.74	810	30.26	17.69	870	28.48	-20.14	1116	24.28	-16.47	839[8]	38.20[13]	n/a

*Data at -32ºC.

In **Table S4** we compare the densities for monomers and dimers of PEG and PPG, obtained with each model against experimental data. For PEG, our model and that of Nawaz yield the best agreement with experiment and show the right trend of increasing density with increasing chain length. For PPG, however, our model shows a density increase with chain length that is too pronounced, leading to a significant overestimation of the PPG density (see also discussion of the micelle density profiles in the main paper). The Nawaz model shows a similar trend, while the best agreement is obtained with the Hakateyama model. Overall, no single model is able to simultaneously reproduce the density of both PEG and PPG moieties.

In **Table S4**, we carried out the same comparison for the enthalpy of vaporization of PEG and PPG. For this property, only experimental data for the dimers were found. Although all models somewhat overestimate the enthalpy for PEG and underestimate that of PPG, our model comes closest to reproducing the latter.

Finally, in **Table S4**, we compare hydration free energies (dG_{sol}) of PEG and PPG monomers and dimers against experimental data (which was only available for the PEG molecules). Although none of the models is very accurate in predicting this property, besides the limitations inherent of CG models to estimate dG_{sol},[14] it is clear that the Hakateyama model leads to PEG moieties that are too hydrophobic (*i.e.* much less favorable dG_{sol} than experimental data). As a consequence, the PEG chains aggregate in water, leading to unrealistic micellar structures (see **Figure S1**). All other models lead to similar PEG hydration free energies, which somewhat overestimate the experimental value. As for PPG, the Hakateyama model has the most hydrophobic beads, again leading to excessive aggregation, while the Nawaz and Hezaveh models both have rather hydrophilic beads. This leads to the PPG chains adopting a stretched conformation in water, preventing their aggregation. Our model, on the other hand, leads to PPG beads

which are mildly hydrophobic. This balance between PEG-water and PPG-water interactions is the main reason for the adequate reproduction of micelle shapes and sizes, as discussed above.

Section S2 – Additional Figures and Tables

In **Figure S2**, we report the cluster size distributions obtained with our cluster counting code for all Pluronic systems. It can be seen that most distributions show a prominent micelle population between 5 and 10 chains, with a tail extending to much larger sizes. This is in qualitative agreement with the polydispersity observed experimentally for these systems, as discussed in the main body of the paper. It is also clear that 31R1 is somewhat of an outlier, showing a nearly exponentially decaying distribution. The reasons for this difference are unclear at present.

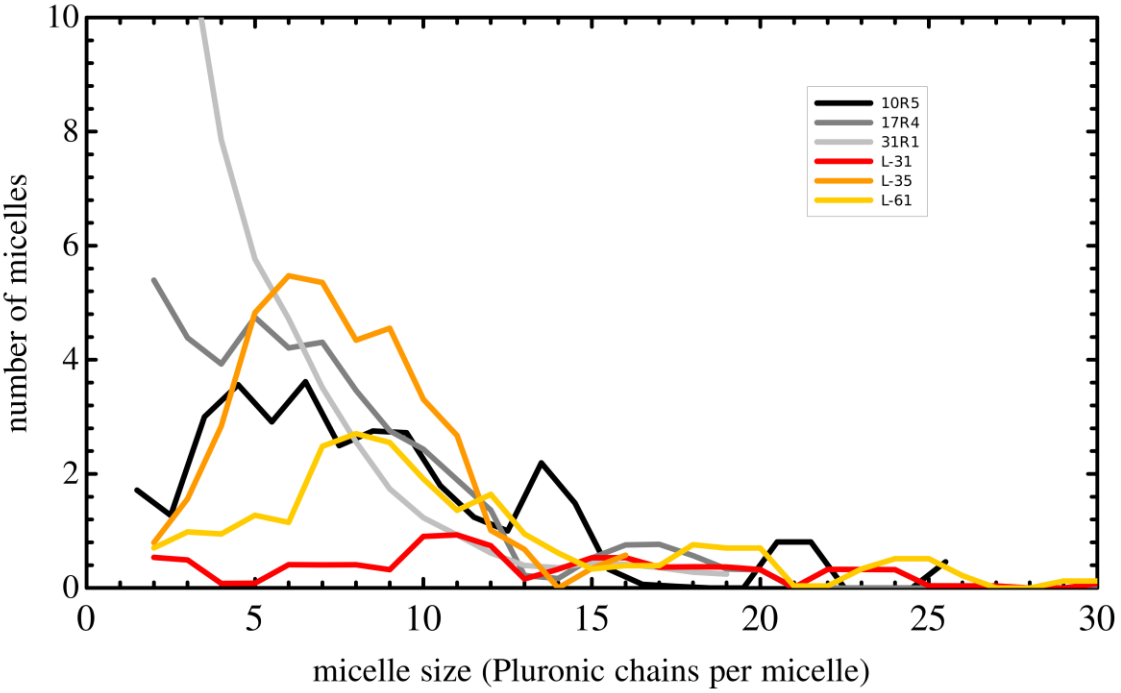

Figure S2. Micelle distribution for all Pluronics obtained with the cluster counting code. The micelle size distribution shows that the averaged micelle size distribution fall in the range of 5 to 15 Pluronic chains *per* micelle. Thus, the micelle distribution was divided in three groups with the most representative micelle size distribution group around 8 chains *per* micelle.

Based on this information, we have divided the micelle size distributions into 3 separate groups: label "8" corresponds to micelles with $N_a < 10$; "15" to micelles with $10 \leq N_a \leq 15$; "20" to micelles with $N_a > 20$. These groups were used in the main body of the paper to discuss the effects of each variable on the thermo-responsive behavior of

Pluronics. Unless otherwise stated, the micelle density profiles shown in the paper were calculated from micelles in the first group, since this was the most heavily populated, in order to compare different systems on the same basis. **Table S5** shows the micelle size distribution for the three micelle distribution groups considered in this work.

Table S5. Average micelle diameter (∅), average aggregation number (N_a), and total number of micelles (N) for each micelle size group. The Pluronic concentration was 1 wt% at the cloud point temperatures shown between brackets.

	10R5 (61°C)			**17R4 (38°C)**			**31R1 (21°C)**			**L-31 (35°C)**			**L-35 (62°C)**			**L-61 (20°C)**		
Groups	**∅**	**N_a**	**N**	**∅**	**N_a**	**N**	**∅**	**N_a**	**N**	**∅**	**N_a**	**N**	**∅**	**N_a**	**N**	**∅**	**N_a**	**N**
8	3.0	7	18	3.3	6	34	3.4	5	47	2.8	10	4	2.7	7	36	3.1	8	15
15	3.7	14	7	4.3	17	3	4.8	17	2	3.2	15	2	3.8	16	1	3.6	16	4
20	3.9	22	3	4.9	25	2	5.2	20	1	3.4	46	5	3.8	17	1	4.0	30	4

In what follows, we present additional results used to complement the discussion in the main body of the paper.

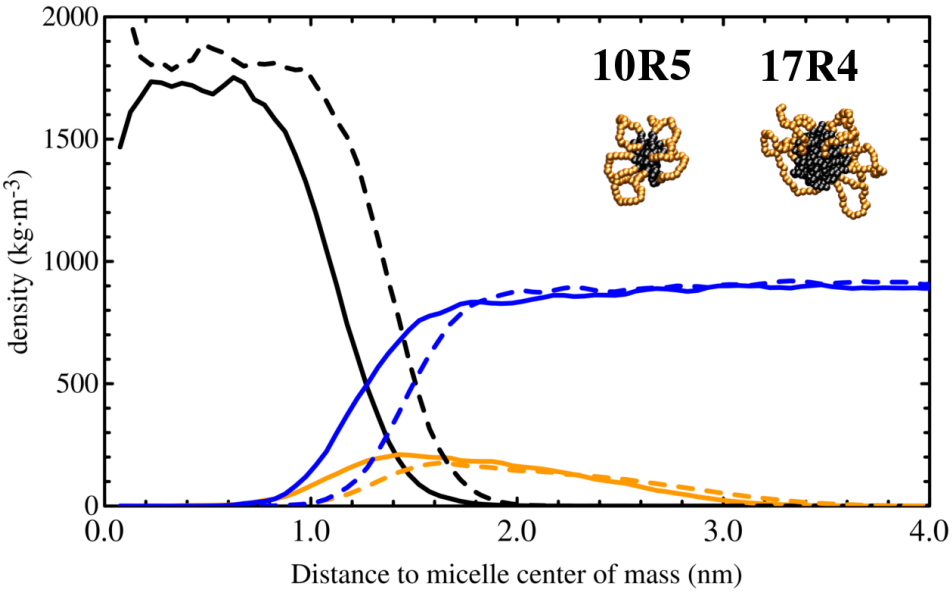

Figure S3. Micelle density profile comparison of 10R5 (solid) and 17R4 (dashed) at 1 wt% of Pluronic concentration at the cloud point temperatures 61°C and 38°C, respectively. The color code is PPG in black, PEG in orange and water in blue.

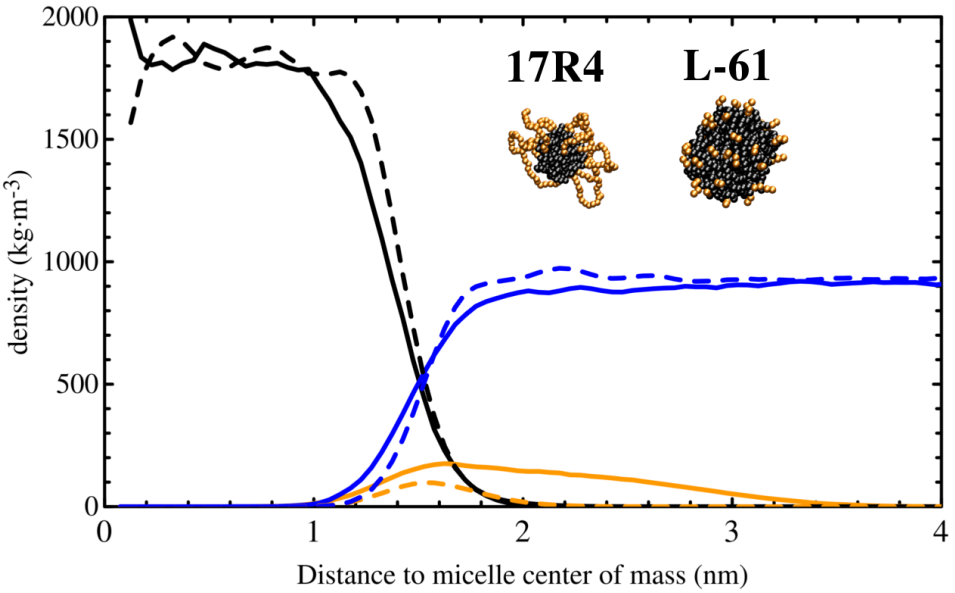

Figure S4. Micelle density profile comparison of 17R4 (solid) and L-61 (dashed) at 1 wt% of Pluronic concentration at the cloud point temperatures 38ºC and 20ºC, respectively. The color code is the same as in **Figure S3**.

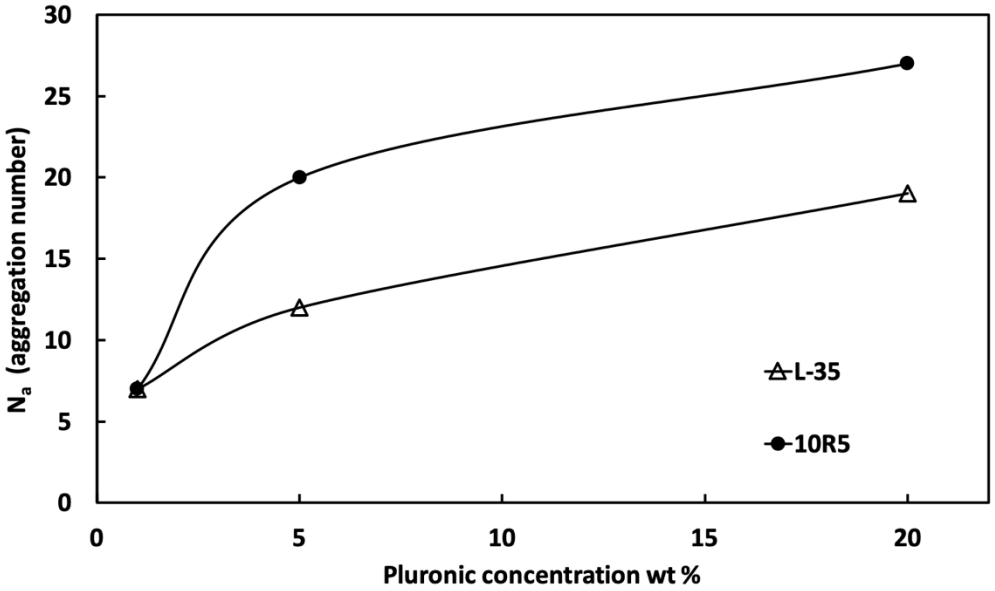

Figure S5. Aggregation number (N_a) of L-35 (Δ) and 10R5 (●) micelles for 1, 5 and 20 wt% of Pluronic concentration at the cloud point temperatures shown in **Figure 10.II**.

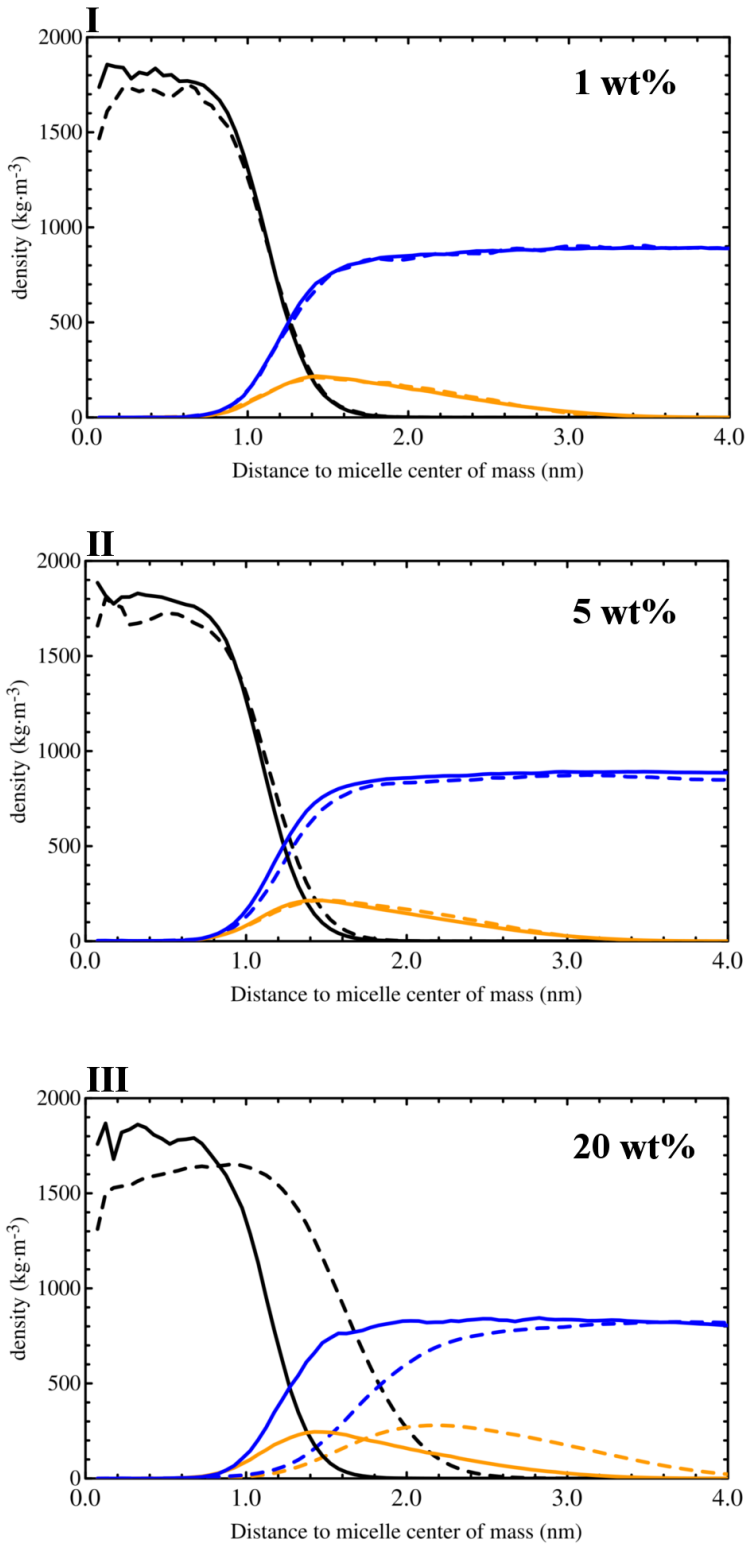

Figure S6. Density profile of 10R5 (dashed lines) and L-35 (solid lines) micelles at (**I**) 1, (**II**) 5 and (**III**) 20 wt% Pluronic concentration. The color code is the same as in **Figure S3**.

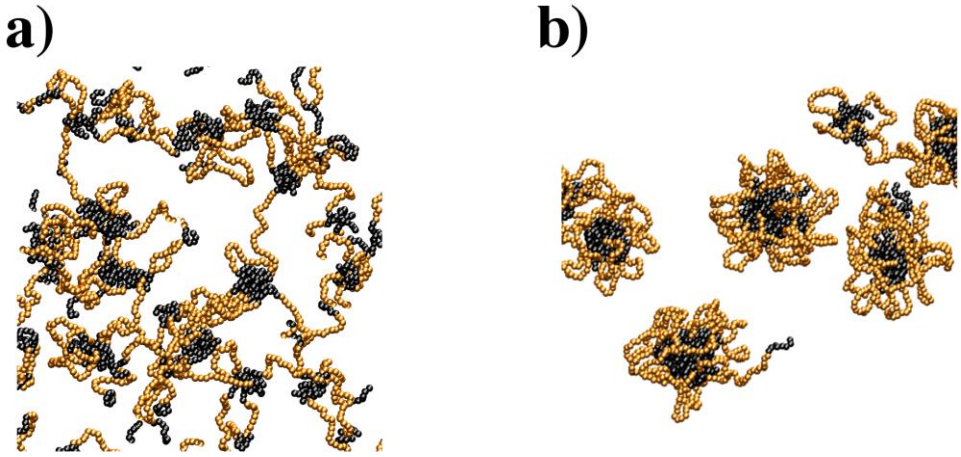

Figure S7. An example of initial stages (**a**) and later stages (**b**) of 10R5 micelle formation obtained in the MD simulations at 1 wt%. In **a)**, isolated 10R5 moieties connect neighboring micelles in the initial micelle formation. In b), the PPG segments belonging to the micelle point outwards from the micelle core and can join the PPG core of close neighbor micelles.

References:

(1) Hezaveh, S.; Samanta, S.; De Nicola, A.; Milano, G.; Roccatano, D. Understanding the Interaction of Block Copolymers with DMPC Lipid Bilayer Using Coarse-Grained Molecular Dynamics Simulations. *J. Phys. Chem. B* **2012**, *116* (49), 14333–14345.

(2) Hatakeyama, M.; Faller, R. Coarse-Grained Simulations of ABA Amphiphilic Triblock Copolymer Solutions in Thin Films. *Phys. Chem. Chem. Phys.* **2007**, *9* (33), 4662.

(3) Nawaz, S.; Carbone, P. Coarse-Graining Poly(Ethylene Oxide)–Poly(Propylene Oxide)–Poly(Ethylene Oxide) (PEO–PPO–PEO) Block Copolymers Using the MARTINI Force Field. *J. Phys. Chem. B* **2014**, *118* (6), 1648–1659.

(4) Nawaz, S.; Carbone, P. Correction to "Coarse-Graining Poly(Ethylene-Oxide)–Poly(Propylene-Oxide)–Poly(Ethylene-Oxide) (PEO–PPO–PEO) Block Copolymers Using the MARTINI Force Field." *J. Phys. Chem. B* **2015**, *119* (7), 3332–3332.

(5) Naskar, B.; Ghosh, S.; Moulik, S. P. Solution Behavior of Normal and Reverse Triblock Copolymers (Pluronic L44 and 10R5) Individually and in Binary Mixture. *Langmuir* **2012**, *28* (18), 7134–7146.

(6) Alexandridis, P.; Alan Hatton, T. Poly(Ethylene Oxide)□poly(Propylene Oxide)□poly(Ethylene Oxide) Block Copolymer Surfactants in Aqueous Solutions and at Interfaces: Thermodynamics, Structure, Dynamics, and Modeling. *Colloids Surfaces A Physicochem. Eng. Asp.* **1995**, *96* (1–2), 1–46.

(7) Pedersen, J. S.; Gerstenberg, M. C. The Structure of P85 Pluronic Block Copolymer Micelles Determined by Small-Angle Neutron Scattering. *Colloids Surfaces A Physicochem. Eng. Asp.* **2003**, *213* (2–3), 175–187.

(8) Daubert, T. E.; Sibul, H. M.; Stebbins, C. C.; Danner, R. P.; Rowley, R. L.; Adams, M. E.; Wilding, W. V; Marshall, T. L. *Physical and Thermodynamic Properties of Pure Chemicals: DIPPR: Data Compilation: Core + Supplements 1-10*; Taylor & Francis, 2000.

(9) Marenich AV, Kelly CP, Thompson JD, Hawkins GD, Chambers CC, Giesen DJ,

Winget P, Cramer CJ, T. D. Minnesota Solvation Database Version 2012. *Minnesota Solvation Database, Univ. Minnesota, Minneapolis.* **2012**, 1–28.

(10) Conesa, A.; Shen, S.; Coronas, A. Liquid Densities, Kinematic Viscosities, and Heat Capacities of Some Ethylene Glycol Dimethyl Ethers at Temperatures from 283.15 to 423.15 K. *Int. J. Thermophys.* **1998**, *19* (5), 1343–1358.

(11) Comuñas, M. J. P.; Baylaucq, A.; Boned, C.; Fernández, J. Volumetric Properties of Monoethylene Glycol Dimethyl Ether and Diethylene Glycol Dimethyl Ether up to 60 MPa. *J. Chem. Eng. Data* **2003**, *48* (4), 1044–1049.

(12) Li, D.; Fang, W.; Xie, W.; Xing, Y.; Guo, Y.; Lin, R. Measurements on Vapor Pressure and Thermal Conductivity for Pseudo-Binary Systems of a Hydrocarbon Fuel with Ethylene and Diethylene Glycol Dimethyl Ethers. *Energy & Fuels* **2009**, *23* (2), 794–798.

(13) Verevkin, S. P. Improved Benson Increments for the Estimation of Standard Enthalpies of Formation and Enthalpies of Vaporization of Alkyl Ethers, Acetals, Ketals, and Ortho Esters. *J. Chem. Eng. Data* **2002**, *47* (5), 1071–1097.

(14) Genheden, S. Solvation Free Energies and Partition Coefficients with the Coarse-Grained and Hybrid All-Atom/Coarse-Grained MARTINI Models. *J. Comput. Aided. Mol. Des.* **2017**, *31* (10), 867–876.